REVIEW

doi:10.1038/nature20416

The activities of amyloids from a structural perspective

Roland Riek[1] & David S. Eisenberg[2,3]

The aggregation of proteins into structures known as amyloids is observed in many neurodegenerative diseases, including Alzheimer's disease. Amyloids are composed of pairs of tightly interacting, many stranded and repetitive intermolecular β-sheets, which form the cross-β-sheet structure. This structure enables amyloids to grow by recruitment of the same protein and its repetition can transform a weak biological activity into a potent one through cooperativity and avidity. Amyloids therefore have the potential to self-replicate and can adapt to the environment, yielding cell-to-cell transmissibility, prion infectivity and toxicity.

The term amyloid describes a particular type of elongated, unbranched protein fibril. It was introduced by physician Rudolf Virchow to describe a macroscopic tissue abnormality with a pale, waxy appearance that produced a positive result — characteristic of starch-like materials — in an iodine-staining reaction; notably, the Latin word for starch is amylum[1]. As defined by pathologists[1] who document amyloids in numerous diseases, the fibrils must be deposited in body tissues and fluoresce a green–yellow colour when stained with the dye Congo red and viewed between crossed polarizers. As defined by biophysical scientists, who also see amyloids as denatured protein aggregates[2–4] and associate them with microbial and cellular functions[5], the fibrils must display the 'cross-β' diffraction pattern caused by the cross-β-sheet motif when irradiated with X-rays (Box 1). The motif is composed of tightly interacting intermolecular β-sheets, and each β-sheet comprises thousands of identical copies of the same β-strand that stack through hydrogen bonding. The backbone amide hydrogen bonds maintain the β-strands at a spacing of 4.8 Å in the direction of the fibril. Two or more such β-sheets lie in parallel, 6–12 Å apart.

The study of amyloids over the past half century has revealed that numerous proteins form amyloid fibrils, some of which are functional and some of which are pathological[6–11]. More than 40 proteins are known to form pathogenic amyloid fibrils[1] and there are at least a dozen functional amyloid fibrils[12,13], with new members of both classes being discovered constantly. Therefore, a fascinating feature of the amyloid state is that a single type of fibril is formed by a wide variety of proteins and is associated with a wide variety of functions — both beneficial and pathogenic. In this Review, our aim is to examine present knowledge of the structures of these fibrils and to establish a structure–activity relationship for amyloid diseases, with a focus on devastating neurodegenerative disorders. Crucial questions include: the extent to which amyloids are the causative entities in the disease process; the mechanisms by which amyloid diseases are transmitted from cell to cell; and the cause of amyloid-induced toxicity.

The cross-β-sheet structure at atomic resolution

Although the cross-β-sheet structure was described 80 years ago and was found to be common to half a dozen different disease-related amyloid fibrils 19 years ago[14], after which it was studied using cryo-electron microscopy (cryo-EM)[15], important questions remained because no atomic-resolution structures were available. One question concerned the features of the cross-β-sheet structure that account for the extreme stability of the amyloid, given that β-sheets form and break up readily. Another question focused on why amyloid fibrils consist generally of a single protein and do not contain mixtures of proteins as would be expected if they were held together mainly by intermolecular backbone hydrogen bonds. Answers emerged from atomic-resolution X-ray structures of amyloid fibrils formed by short peptide segments of amyloid-forming proteins[16–26]. These structures were enabled by the discovery that such fibril-forming segments also form needle-shaped microcrystals in which the amyloid protofilaments span the entire length of the crystals[27].

The atomic-resolution X-ray structures reveal that the basic cross-β-sheet motif consists of a pair of tightly mating repetitive β-sheets (Fig. 1 and Box 1). When viewed along the axis of the protofilament, the two β-sheets adhere by the interdigitation of the side chains of the mating strands, much like the teeth of a zipper. For this reason, the dual-sheet motif is termed a 'steric zipper'. The interface between the two sheets in almost all cross-β-sheet structures is devoid of water. The intricate interlacing of the side chains shows that the formation of the fibrils depends on the sequence of the participating segments. That is, the segments that form these structures are self-complementary. The stability of the fibrils arises from several factors. One such factor is the hydrogen bonds that form between backbone amide groups that run up and down the β-sheets. Because each amide hydrogen bond is polar, lines of parallel hydrogen bonds pointup and down the β-sheets. In this arrangement, the hydrogen bonds polarize one another, which creates a cooperative energy of formation[28]. Another factor is the van der Waals forces that form between the closely interacting pairs of β-sheets. A third factor is the increase in entropy of the water molecules that are released from the inner faces of the two β-sheets that meet so closely. And a further stabilizing factor is the interaction of side chains that run up and down the β-sheets. Interacting side chains include Tyr aromatic rings that stack because of π–π interactions. Side chains of Asn, Gln, Thr and Ser form hydrogen bonds known as ladders, which run up and down the fibrils (for example, the Gln ladder in Fig. 1) (refs 16 and 17).

All amyloid-segment microcrystals show that the cross-β-sheet motif is composed of two, almost infinite, β-sheets with a steric-zipper side-chain interface. However, the various cross-β-sheet structures can be categorized according to several criteria: whether their β-strands are parallel or antiparallel; whether their β-sheets pack with the same surfaces (face-to-face packing) or different surfaces (face-to-back packing) adjacent to one another; and, whether the two closely packed β-sheets

[1]Laboratory of Physical Chemistry, Department of Chemistry and Applied Biosciences, ETH Zurich, 8093 Zürich, Switzerland. [2]UCLA-DOE Institute, Los Angeles, California 90095-1570, USA. [3]Howard Hughes Medical Institute, Los Angeles, California 90095-1570, USA.

© 2016 Macmillan Publishers Limited, part of Springer Nature. All rights reserved.

BOX 1

The cross-β-sheet motif

Amyloids are composed of an ordered, repetitive arrangement of many (usually thousands) copies of a peptide or protein (Box Fig., array of arrows). The repeating substructure consists of two layers of intermolecular β-sheets that run in the direction of the fibre axis. Amyloid fibrils can be identified easily using electron microscopy as long, unbranched filaments with diameters of 6–12 nm (ref. 129). The cross-β-sheet motif gives rise to characteristic X-ray fibre diffraction patterns with a meridional reflection at about 4.8 Å, which corresponds to the spacing between β-strands, and a protein-dependent equatorial reflection at 6–12 Å, which corresponds to the distance between stacked β-sheets[14,130] (an example spacing of 10 Å is shown in the Box Fig.). The cross-β-sheet motif was first described in 1935 by William Astbury, who measured the X-ray diffraction pattern of stretched, poached egg white[130].

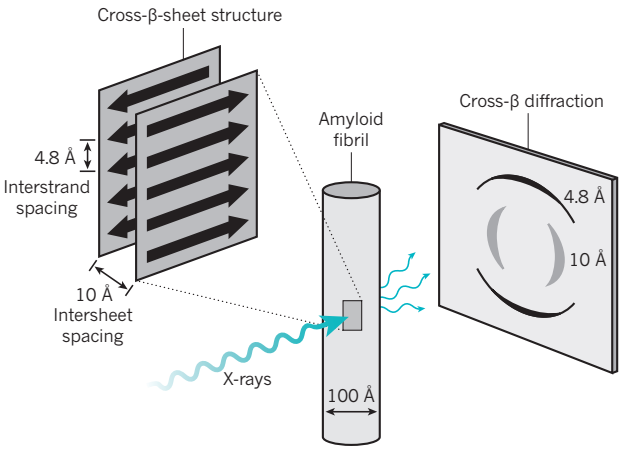

are oriented in the same direction (up–up) or opposite direction (up–down). Combinations of these three structural arrangements give eight theoretically possible classes of steric zippers, seven of which have now been seen in X-ray structures[29] (Fig. 1). Whether the β-strands in a β-sheet are parallel or antiparallel to each other, they are generally in register. This means that in a parallel β-sheet, each β-strand lies exactly above the β-strand below, and in an antiparallel β-sheet, each β-strand lies exactly above the β-strand that is two strands below. Out-of-register β-sheets have been seen in X-ray structures but are rare[24,30].

The amyloid peptide crystal structures that we discuss indicate the prevalence of the cross-β-sheet motif with steric-zipper-type side-chain interactions in peptide complementation and oligomerization in amyloid fibrils. However, an important consideration is the extent to which the structures of amyloid fibrils generated from segments of amyloid-forming proteins represent the fibril structures that are formed by their full-length parent proteins[31].

3D structures of amyloid-β, α-synuclein and HET-s prion

The relevance of the steric-zipper structures is supported by the observation of such a motif in a cryo-EM structure of amyloid-β(1–42), which is a full-length amyloid fibril[32]. However, two — essentially identical — structures of amyloid-β(1–42) fibrils determined by solid-state nuclear magnetic resonance (NMR) show that other types of interactions are also present[33,34] (Fig. 2). In these structures, there are also two peptides per layer of the protofilament axis, but each layer now contains two complete amyloid-β(1–42) peptides. Although residues 1–14 of each peptide are poorly ordered, residues 15–42 form a double horseshoe shape, which resembles the letter S (ref. 35). Each peptide contains four β-stands that stack on top of identical β-strands along the axis to form in-register, intermolecular β-sheets. Pairs of these strands interact with interdigitating or abutting side chains, but the pair members differ in sequence (Fig. 2b). Therefore, these zippers are heterosteric zippers, unlike the homosteric zippers that are found in the amyloid segments of the X-ray structures. Furthermore, each peptide has sharp bends at its Gly residues and contains two hydrophobic cores, an Asn ladder, a Gln ladder and a salt bridge between the side chain of Lys28 and the C terminus[35], and its polar side chains face the solvent on the periphery of the protofilament. The two peptides of each layer meet at a two-fold axis (Fig. 2c) in a homosteric-zipper-like interaction; however, because each peptide contributes two segments to the zipper, it is a non-contiguous zipper interaction. Overall, the complexity of the fold seems to be dictated by the degree to which hydrophobic side chains can be buried, which also drives the folding of soluble proteins. Unusual structural features can arise from the energetic drive to bury hydrophobic side chains in structures that have not evolved to perform functions. Examples of these include sequential aromatic side chains (Phe19 and Phe20) that both face the hydrophobic core, and two negatively charged side chains (Glu22 and Asp23) in concert with Ala21 that face the solvent.

A 3D structure of α-synuclein amyloid fibrils, which are pathogenic in neurons and are associated with Parkinson's disease (PD), has been determined by solid-state NMR[36] (Fig. 3a). The core structure (residues 46–94) has an orthogonal Greek-key topology. It is composed of several parallel, in-register cross-β-sheets with heterosteric-zipper side-chain interactions such as hydrophobic interactions, aromatic π–π stacking (Phe94) and glutamine ladders (for example, Gln79). It is flanked by less-structured N-terminal and C-terminal segments of more than 40 residues in length.

So far, no high-resolution structure of a mammalian prion in the amyloid state has been determined. A low-resolution electron tomography study of infective prion fibrils from the brain of a mouse has revealed paired protein fibrils[37] and a cryo-EM study of the infectious variant of prion protein (PrP^{Sc}) from a mouse suggests that each molecule of PrP^{Sc} has a β-solenoid structure with four layers[38]. By contrast, solid-state NMR experiments suggest that fibrils of recombinant PrP^{Sc} have a parallel in-register, intermolecular β-sheet architecture[39–42]. In the absence of atomic-level information on mammalian prions, the high-resolution structure of the amyloid of infectious prion HET-s is noteworthy for its further elements of fibril architecture. HET-s is a functional prion from the filamentous fungus *Podospora anserina* and is involved in a primitive immune system[43]. The 3D structure of the infectious HET-s(218–289) fibrils determined by solid-state NMR reveals a left-handed β-solenoid that is composed of four in-register parallel β-sheets[44] (Fig. 3b). Each protein molecule contributes two windings of a helix to the length of the fibril so that the β-strands alternate between intermolecular and intramolecular hydrogen bonding along the axis of the fibre. The interior of the β-solenoid is composed of a hydrophobic core as well as Thr–Ser and Asn ladders, and the solvent-exposed face consists mostly of polar and charged side chains forming a pattern of alternating charges along the fibril axis that is enabled by the fibril's two-layer architecture. Notably, mammalian PrP^{Sc} also seems to be composed of a β-solenoid but with four windings per molecule[35,45].

Structural polymorphism of amyloids

Amyloid polymorphism is a phenomenon in which a given peptide or protein sequence adopts two or more structurally distinct conformations of amyloid under the same environmental conditions. At the mesoscopic level, amyloid polymorphs can be identified using the features of their fibrils, including fibril morphologies (such as the ribbons or twisted fibrils of α-synuclein)[46,47], the degree of twist in the fibril, the number of protofilaments per fibril and the diameter or mass per unit of fibril length[48], or by the detection of numerous signals per atom in solid-state NMR spectra[47,49–52]. At the atomic level, insights into the basis of the structural pluralism of amyloids can be obtained from

© 2016 Macmillan Publishers Limited, part of Springer Nature. All rights reserved.

crystal structures of amyloid peptides (Fig. 4). For example, for the peptide segment KLVFAA (residues 16–21) of amyloid-β(1–42), three steric zipper cross-β-sheet motifs were found (Fig. 4a–c) and for the peptide segment MVGGVVIA (residues 35–42), two structures were found[21] (Fig. 4d, e). On the basis of these structures, such polymorphisms can be classified as segmental polymorphs in which different segments form the cross-β-sheet cores of the two polymorphs, or as packing polymorphs in which the same segment forms the cross-β-sheet core but is packed differently (such as parallel strands versus antiparallel strands or alternative steric-zipper side-chain interactions)[20]. At the mesoscopic level, polymorphisms can occur through different modes of binding between the protofilaments in a fibril. These weak, local interactions gain avidity by their summation over thousands of identical copies along the axis of the fibril. Such different supramolecular structures might be the result of underlying packing or segmental polymorphisms at the atomic level or could themselves be an independent form of polymorphism, termed an assembly polymorphism[51]. The number of amyloid polymorphs of a protein depends on the protein and can be estimated crudely as varying between a few and a few dozen[9,50].

Amyloid polymorphism might seem to challenge Christian Anfinsen's thermodynamic hypothesis, which describes a one-to-one correlation between a polypeptide sequence and its 3D structure[53]. However, Anfinsen stated his hypothesis applies to the structures of native proteins in their normal physiological milieu, in which the native state is the lowest free-energy state under the given conditions. Pathogenic amyloid sequences are not in their native states when they form amyloid fibrils and, because they change conformation to reach the amyloid state, probably pass outside of their normal physiological milieu. Amyloid sequences that form pathogenic fibrils have not experienced evolutionary optimization, unlike functional amyloids[54], which can yield energetically similar but distinct structures that are separated from one another by energy barriers larger than thermal energy. Furthermore, even a less stable polymorph can be the predominant species in a sample. This is because the aggregation of amyloid is initiated by stochastic nucleation and aggregates grow by kinetic processes in which the polymorph can replicate itself more quickly than a more stable polymorph. Together, these factors result in a plethora of kinetically uncoupled alternative structural states. For this reason, the collection of amyloid aggregates in an infected organism might comprise a pool of polymorphs with condition-dependent relative abundancies. Because these polymorphs are structurally distinct, they could also have different activities. This is exemplified by the atomic-resolution structures shown in Fig. 4. The intersheet steric-zipper motifs between the polymorphs differ, yielding distinct amyloid stabilities, and correspondingly, the surfaces between the polymorphs require dissimilar interaction activities[55].

General properties of amyloids

Two general biochemical properties account for the biological effects

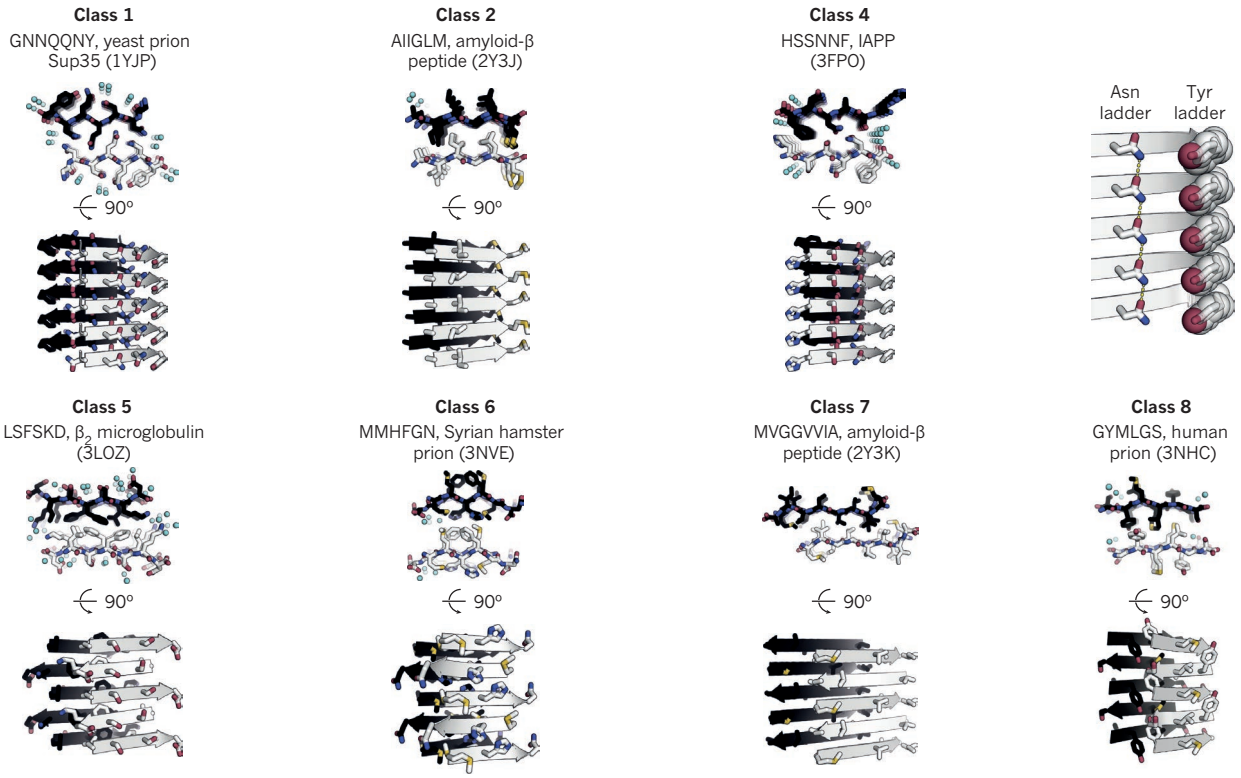

Figure 1 | Atomic-resolution X-ray diffraction steric-zipper structures of amyloid protofilaments formed by short segments of amyloid-forming proteins. Each structure illustrates one of the possible symmetry classes of steric zippers, with views along (top) and perpendicular to (bottom) the protofilament axis. One β-sheet is shown in black and the other is in grey. Notably, water molecules (light blue spheres) are excluded from the tight interface between the β-sheets. Nitrogen atoms (blue), oxygen atoms (red), sulfur atoms (yellow) and β-strands (arrows) are depicted. For each class, the amino-acid sequence of the representative segment, the parent protein from which the segment was selected and the Protein Data Bank (PDB) accession code (in parentheses) for the coordinates of the structure is presented. Classes 1, 2 and 4 (top row) describe parallel β-sheets and classes 5–8 (bottom row) describe antiparallel β-sheets. Asn and Tyr ladders are also shown (top right). Class 3 has not yet been observed experimentally. Each class is defined on the basis of several characteristics: whether their β-strands are parallel or antiparallel; whether their β-sheets pack with the same (face-to-face) surface or different (face-to-back) surface adjacent to one another; and, whether the two closely packed β-sheets are oriented in the same (up–up) direction or the opposite (up–down) direction. In summary: class 1 contains parallel, face-to-face, up–up structures; class 2 contains parallel, face-to-back, up–up structures; class 3 contains parallel, face-to-face, up–down structures; class 4 contains parallel, face-to-back, up–down structures; class 5 contains antiparallel, face-to-face, up–up structures. Class 6 contains antiparallel, face-to-back, up–up structures; class 7 contains antiparallel, face-to-face up–down structures; and, class 8 contains antiparallel, face-to-face, up–down structures. IAPP, islet amyloid polypeptide.

© 2016 Macmillan Publishers Limited, part of Springer Nature. All rights reserved.

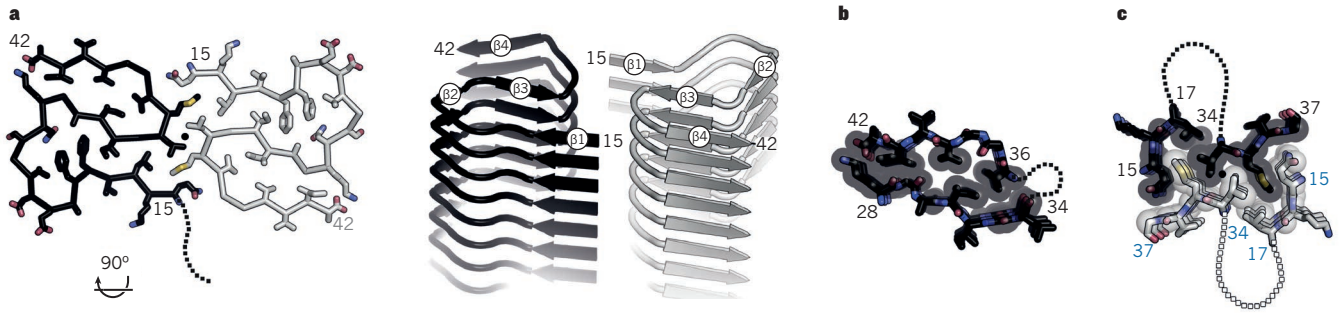

Figure 2 | Solid-state NMR structure of the ordered portion of the amyloid fibril formed by the AD-related peptide amyloid-β(1–42). **a**, Views along the axis of the protofilament of amyloid-β(1–42) (left) and almost perpendicular to the same protofilament (right). Two essentially flat molecules in each layer of the protofilament are related by a two-fold axis (black circle). Each molecule has the shape of a double horseshoe, or an inverted letter S, and is stabilized by hydrogen bonding to molecules both above and below, as well as by several heterosteric zippers. **b**, Example of a stabilizing heterosteric zipper. Note the tight packing of the side chains at the interface between the two segments of the zipper. **c**, The homosteric zipper that forms between the two molecules across the two-fold axis. Amino-acid residues from each molecule that contribute to the zipper interaction are not contiguous in the protein chain. In **b** and **c**, dotted lines represent intervening residues. Adapted with permission from ref. 128.

of amyloids. The first is that amyloid-forming proteins can switch from soluble monomers to insoluble fibrils (Box 2). This change of phase can disrupt the function of cells and organs, through either the loss of a crucial function or the gain of a toxic function. For example, the tumour-suppressor function of p53 is lost through p53 aggregation[56–59]. And the HET-s prion induces refolding of the soluble HET-S prion into a membrane protein that induces a necroptosis-related, spatially limited cell death in *Podospora anserina*[60,61].

The second property is the repetitive structure of amyloids. Because the cross-β-sheet structure is built mostly of intermolecular contacts, the initial formation of amyloid is governed by a high concentration of amyloid protein, and after aggregation has been triggered (Box 2), amyloids might persist indefinitely (such as in the cases of the HET-s prion, which persists in nature[60], and the amyloids that are proposed to be involved in memory[62–64]). Because of the subnanometre repetitiveness of the structure, a non-specific activity such as (inappropriate) ligand binding can be amplified into a potent effect through avidity or cooperativity. Its repetitive configuration also endows amyloids with a capacity to bind to other repetitive biomolecules such as RNA, DNA, glycosaminoglycans and lipid membranes with a relatively high affinity[55,65,66]. The structural repetitiveness of the amyloid fibre provides an ideal template for replication and might therefore be transmissible between cells — or even infectious in the case of prion diseases[67].

Replication and transmission of amyloids

The repetitive nature of amyloids is the basis of their capacity for templating identical structures through the recruitment of identical soluble protein molecules, therefore replicating themselves (Fig. 5). Replication depends on the concentrations of soluble and aggregated amyloid proteins, the rate of growth of the amyloid and the rate of breakage of the amyloid fibre into seeds, and it might also depend on so-called secondary nucleation steps such as amyloid aggregation that is catalysed on the surface of the side of the fibril[68–70]. According to this theoretical framework, manipulation of these variables affects the growth and replication of amyloids[71]. For example, an increase in the levels of soluble amyloid protein in the host might be sufficient for the replication and spread of amyloid-β aggregates *in vivo* on inoculation with seed material (that is, amyloid templates)[72], and the chaperone protein Hsp104, which has the ability to fragment fibrils of the Sup35 prion into smaller pieces, is required for prion propagation in yeast[73].

Prions are the prototypical amyloids with *in vivo* replication properties. The 'protein-only' hypothesis[74–76] states that prion diseases, including scrapie in sheep, bovine spongiform encephalopathy (BSE) in cattle and Creutzfeldt–Jakob disease in humans, can be distinguished from infectious diseases that are caused by bacteria, viruses or viroids. Prion diseases originate and propagate through the conformational conversion of normal cellular prion protein (PrP^{C}) into PrP^{Sc} (ref. 67), an altered β-sheet-rich — and usually protease-resistant — form of PrP that is now known to be an amyloid entity. The amyloid serves as an infectious seed, which recruits soluble host PrP^{C} for growth. The growing amyloid can fragment to produce further infectious seeds, which means that prions are essentially infectious proteins. Prions have been identified in lower eukaryotes, namely yeast and *Podospora anserina*[43,77–80], as well as in mammals, and recombinant protein production has been used to show that the amyloid of a corresponding prion protein can be infectious in several of the kingdoms of life[81–83].

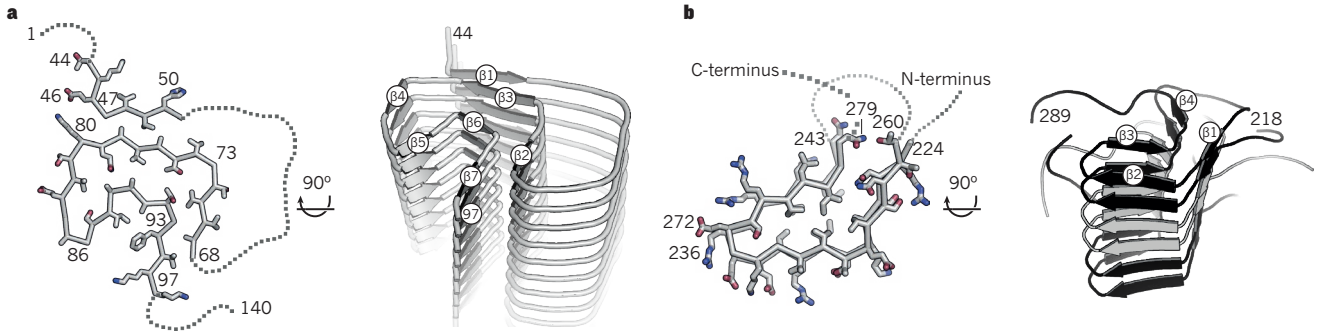

Figure 3 | 3D structure of the cores of the α-synuclein fibrils and the HET-s(218–289) prion. **a**, Views along the axis of the protofilament of α-synuclein (left) and almost perpendicular to the protofilament (right) (PDB accession code 2N0A). The overall architecture of the core of α-synuclein fibril comprising residues 44–97 is shown with nine molecules using a ribbon representation; β-strands are indicated (right). **b**, Views along the axis of the protofilament of the HET-s(218–289) prion (left) and almost perpendicular to the protofilament (right). The overall architecture of the HET-s(218–289) prion fibril is shown with three molecules using a ribbon representation; the molecules are coloured black or grey and arrows indicate β-strands. Each molecule makes two windings in the β-solenoid structure.

© 2016 Macmillan Publishers Limited, part of Springer Nature. All rights reserved.

Given the ability of amyloids to replicate, it is possible that amyloids other than prions might also spread from cell to cell *in vivo*, as well as from organism to organism. Cell-to-cell spreading of several disease-associated proteins in the amyloid state has been confirmed in laboratory animals[84], but see Walsh and Selkoe[85]. Such amyloids include amyloid-β[72,86,87], which is associated with Alzheimer's disease (AD), and α-synuclein[88]. The transmission of disease symptoms between mice has been shown for the amyloid-related condition amyloid A (AA) amyloidosis[89]. Furthermore, there is considerable evidence to suggest that the accumulation of amyloid-β was induced in people through treatment with growth hormone prepared from large pools of cadaver-derived pituitary glands[90] and that brain homogenates from deceased people with AD induced the formation of plaques in marmosets[91]. The cellular spread of amyloid-β is supported further by the presence of a single amyloid-β polymorph in different regions of the brain in people with AD[92]. Although amyloid replication *in vivo* and its transmissibility are evident in many cases, it must be noted that, with the exception of prion diseases and systemic amyloidosis, the clinical symptoms of the diseases in these settings have been mostly missing[93,94].

Prion strains

In mammals, more than a dozen strains of prion are known[95]. Prion strains are distinguished by several phenotypes, including the length of incubation, the ability to cross a species barrier and the area of the brain in which PrP is deposited. Because PrP in its aggregated conformation is the infectious culprit of prion diseases (according to the protein-only hypothesis), the strain-specific properties must be attributed to altered conformations of PrP amyloids. On this basis, it is straightforward to propose that several distinct structural polymorphisms yield various forms of amyloid with distinct activities. Indeed, mammalian prion strains can be differentiated through patterns of PrP glycosylation[96], conformation-selective PrP antibodies[97], fluorescent dyes that bind to specific amyloid conformations[98] and PrP resistance to protease[99]. Furthermore, amyloids of the yeast prion Sup35 with distinct conformations can be propagated *in vitro* to produce several distinct strains of prion on infection[68,100]. Specifically, two polymorphs of Sup35 fibrils lead to different strains of prions with distinct cross-β-sheet cores[101].

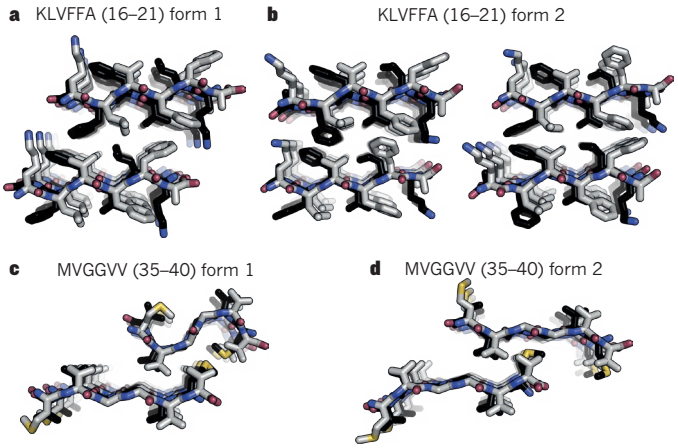

Figure 4 | Polymorphic atomic-resolution X-ray structures of amyloid fibrils formed by fragments of amyloid-β, viewed along the axes of the fibrils. **a**, **b**, Three polymorphic protofilaments of a segment of amyloid-β with the sequence KLVFFA (residues 16–21). Actual fibrils have tens of thousands of layers but only four layers are shown. Alternating layers are coloured black and grey. **c**, **d**, Two polymorphic protofilaments of a fragment of amyloid-β with the sequence MVVGGVV (residues 35–40). Note that all β-sheets are antiparallel[21].

Adaptation of amyloids

Strain adaptation is observed in prion diseases. For example, the adaptation of a prion strain to a new host results in a decrease in the time to the onset of symptoms for the first few serial transmissions. Several studies provide further evidence that prions are able to adapt to a new cellular environment[102–104]. In the presence of the drug swainsonine, a population of prions that were resistant to swainsonine emerged. Interestingly, after the drug was withdrawn, drug-sensitive prions appeared again. These findings indicate that the infectious material is composed of a pool of several prion polymorphisms, some of which are present only at very low levels. However, one such polymorphism might replicate more efficiently when the environment changes, becoming the predominant

BOX 2

Amyloid aggregation

A simplified mechanism of the nucleation-dependent process of amyloid aggregation[75,118,131–133] is shown in the Box Fig. For aggregation to be initiated, the soluble amyloid proteins or peptides (blue coils) must be partially unfolded, misfolded or intrinsically disordered. Furthermore, several molecules must come together to form a nucleus (star-like entity composed of several extended blue coils) from which the amyloid can grow. Because the nucleus is the most energetically unfavourable state, nucleus formation seems to determine the reaction rate. After the nucleus has formed, the further addition of monomers becomes faster, favouring growth of the aggregate (arrays of extended blue entities). Evidence from experiments indicates that such nuclei could be oligomers of a different structural nature to that of the final amyloid fibrils (arrays of blue arrows). There might be further intermediates such as protofibrils (array of arrowless, extended blue entities) that finally become amyloid fibrils (array of blue arrows). Some fibril formation *in vitro* might also be driven by the artificial water–air interface[134,135] or could include helical intermediate states. Secondary nucleation processes, including fibril fragmentation and nucleus formation induced at the amyloid fibril surface[69,70,136], are of particular relevance to the kinetics of fibril growth. Off-pathway aggregation might also occur. Notably, other mechanisms of aggregation such as downhill polymerization of transthyretin[137] can occur.

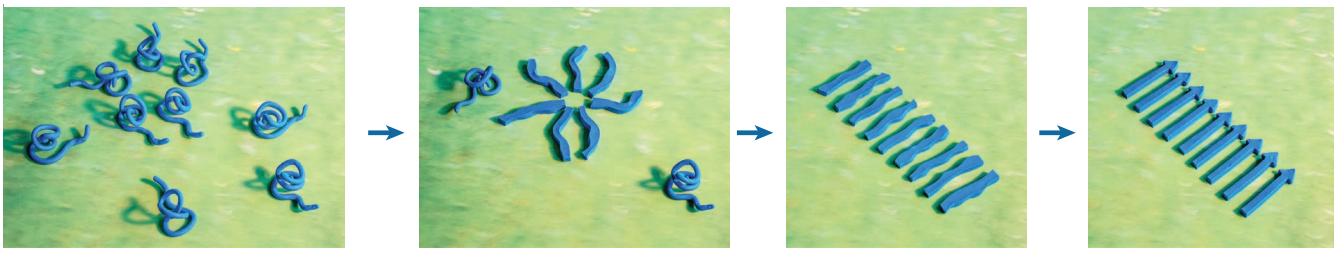

© 2016 Macmillan Publishers Limited, part of Springer Nature. All rights reserved.

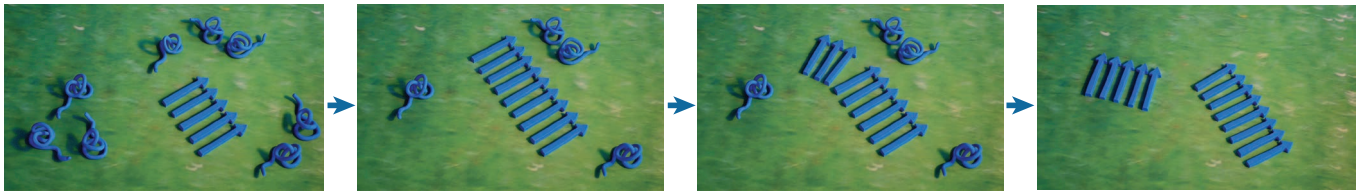

Figure 5 | The replication of amyloids. An amyloid seed (array of five blue arrows) recruits soluble amyloid protein (blue coils) and expands. The growing amyloid might fragment, which generates two seeds and therefore increases the number of replicative entities (arrays of five and eight arrows). The green background represents a given environment.

species[105,106] (Fig. 6). Even in the absence of a polymorph that is suited to the environment, a new polymorph could emerge through a *de novo* nucleation-dependent process of amyloid aggregation. Therefore, a species of amyloid protein has the potential to self-replicate after it has aggregated and can adapt to its environment, which suggests that it might evolve in a non-Mendelian fashion.

Toxicity of amyloids

Although the pathological properties of amyloid load and propagation can be understood from the structural and physical–chemical properties of amyloids, the mechanism of amyloid toxicity in neurodegenerative diseases remains unknown. The association of amyloid fibrils with disease is strong: aggregates of amyloid-β are found in plaques associated with AD; tau aggregates are found in neurofibrillary tangles that are also associated with AD; α-synuclein fibrils are the main protein in Lewy bodies, the histological hallmark of PD[107]; and protease-resistant amyloid fibrils are found in prion diseases. Also, familial amyloid diseases are characterized by mutations that favour aggregation by enhancing either the production of the amyloid protein[108–110] or by stabilizing the amyloid structure, as evident from the 3D structure of the amyloid-β(1–42) amyloid (Fig. 2). All familial mutations in the amyloid-β(1–42) sequence (that is, Lys16Asn, Ala21Gly, Glu22Gln, Glu22Gly, Glu22Lys, Glu22Δ and Asp23Asn) are located at the structurally frustrated segment Ala20–Asp23, and most of these mutations are expected to release this frustration, at least partly. Although many of the mutations (Lys16Asn, Glu22Gln, Glu22Gly, Asp23Asn and Glu22Lys) probably attenuate intermolecular charge repulsion, Ala21Gly and Glu22Gly might instead relax the backbone restraints, owing to the peculiar side-chain arrangements of the segment Phe19–Asp23. Furthermore, in the rare familial neurodegenerative disease diabetes insipidus, amyloid aggregation of the prohormone provasopressin in the endoplasmic reticulum causes endoplasmic reticulum stress that results in cellular death[111]. Consequently, the amyloid state is associated strongly with disease. However, its association with direct cytotoxicity is less strong. The anchorless PrP^{Sc} is highly infectious without causing toxicity[112], and in other mammalian prion systems, the infectivity titre and toxicity seem to be uncoupled[113]. Furthermore, there seems to be a weak correlation between amyloid load and toxicity in AD[114].

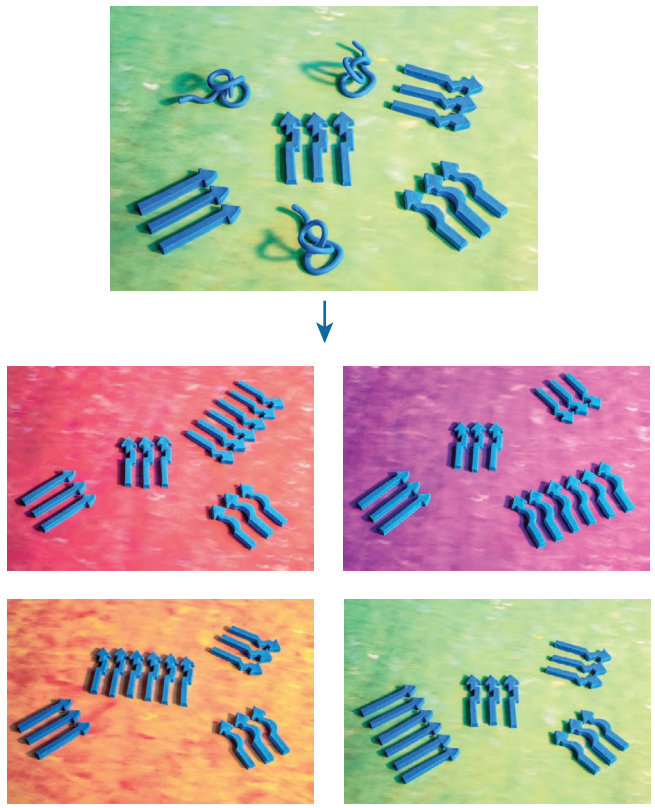

Figure 6 | The adaptation of amyloids to various environments. Four different amyloid polymorphs (arrays of three polymorph-specific blue arrows, top) are surrounded by soluble amyloid protein (blue ribbons). When the environment is changed (red, pink or orange background) mainly one of the four polymorphs continues to grow, and each set of environmental conditions selects a different polymorph for expansion. With time, the growing polymorph becomes most abundant.

On the basis of these apparently inconsistent data, the following five hypotheses on the origin of toxicity have been proposed. First, amyloid fibrils are the toxic entities, as stated in the amyloid cascade hypothesis[115–118]. For example, on the basis of the high-resolution structure of amyloid-β(1–42) fibrils, it is difficult to imagine that the presence of the hydrophobic repetitive patches of Val40–Ala42 flanked by Lys28 or Val18–Ala21 flanked by Arg16, which run along the surface of amyloid-β(1–42) amyloids (Fig. 2) are without consequences for cell viability. Such regions might bind to other proteins tightly and without specificity through hydrophobic interactions or perturb or integrate, in part, with membranes.

Second, amyloid oligomers are the toxic entities. These are smaller aggregates of the same proteins that go on to form fibrils[114,119,120] (Box 2). Amyloid fibrils might catalyse the formation of toxic oligomers through their surfaces[69,121] and could be the agents for cell transmission. This would make fibrils an important, although indirect, component of the mechanism of toxicity.

Third, other oligomers off the pathway to fibrils are the toxic entities. An example is cylindrin[122], which might perturb the integrity of the cellular membrane by insertion. In this hypothesis, the amyloid fibril is a non-toxic entity that enables the cell to escape the toxicity caused by the oligomers.

Fourth, a process — rather than a specific structural state — accounts for the toxicity. That is, the mechanism of fibril growth *per se* is the toxic process[123,124]. This hypothesis is supported by the finding that during the aggregation of α-synuclein on a lipid membrane, lipids are extracted by the growing fibril, whereas adding a fibril to a lipid bilayer merely results in binding of the amyloid to the membrane[124].

Last, cellular stress accounts for the toxicity. The so-called neuronal vulnerability hypothesis states that neurodegenerative diseases spread in an organism: concomitantly, aggregation of the amyloid protein is a cellular stress that is transferred from cell to cell. The cellular stress not only degrades the cell but also induces *de novo* aggregation[85].

When weighing up the various hypotheses, it must be noted that several amyloid polymorphs and various amyloid oligomers might be

© 2016 Macmillan Publishers Limited, part of Springer Nature. All rights reserved.

present in an affected individual and that each of these structural entities or mechanisms of aggregation could have distinct toxicity-related activities. The diseases might therefore be caused by several of these structural entities and processes, which would account for the complex, multifaceted nature of amyloid diseases that has been documented.

Given the limited fidelity of animal models to human diseases, tracing mechanisms of toxicity is especially challenging. Seeking chemical or biological interventions on the basis of structural and physical–chemical considerations might help to elucidate the structure–toxicity relationship in amyloid diseases. Possible approaches to intervention[125] include: the prevention of amyloid elongation through use of structure-based inhibitors (such as ref. 58); the inhibition of secondary nucleation[121,126]; the inhibition of amyloid nucleus or oligomer formation; the inhibition of amyloid oligomer membrane insertion; the inhibition of amyloid spreading between cells; and, the inhibition of amyloid formation through the stabilization of native structures. The structures of the amyloids might therefore be used in the rational design of molecules for disease intervention. For example, the hydrophobic hot spot around Phe19 and Phe20 in the structure of amyloid-β(1–42) (Fig. 2) is a potential interesting pharmacophore for the inhibition of fibril elongation. The epitopes comprising residues Val40–Ala42–Lys28 or Leu17–Ala21–Arg16 form surface-exposed hydrophobic patches that are flanked by a positive charged ladder, indicating that they are involved in secondary nucleation or membrane interaction and making them prime candidates for intervention in these processes. Disease intervention through the stabilization of a native structure has yielded a drug for the condition transthyretin amyloidogenesis (reviewed in ref. 127). This physico-chemical approach, termed kinetic stabilization, is built on the hypothesis that the formation of amyloids causes disease and that amyloid aggregation can be inhibited by stabilizing the folded native tetramer of the protein transthyretin[45]. Remarkably, this approach enabled discovery of the drug tafamidis without the availability of good animal models of transthyretin amyloidogenesis. Tafamidis was recently approved by the European Medicines Agency for the treatment of transthyretin familial amyloid polyneuropathy. This example illustrates how a thorough understanding of the mechanism of aggregation of the soluble state of an amyloid protein can lead to a treatment for amyloid-based disease. Furthermore, it is a prime example of the establishment of a drug based purely on physical–chemical principles and studies and it is the first drug that has been approved to treat an amyloid disease. ■

Received 1 August; accepted 14 September 2016.

1. Sipe, J. D. *et al.* Nomenclature 2014: amyloid fibril proteins and clinical classification of the amyloidosis. *Amyloid* **21,** 221–224 (2014).
2. Gustavsson, A., Engström, U. & Westermark, P. Normal transthyretin and synthetic transthyretin fragments form amyloid-like fibrils *in vitro*. *Biochem. Biophys. Res. Commun.* **175,** 1159–1164 (1991).
3. Colon, W. & Kelly, J. W. Partial denaturation of transthyretin is sufficient for amyloid fibril formation *in vitro*. *Biochemistry* **31,** 8654–8660 (1992).
4. Booth, D. R. *et al.* Instability, unfolding and aggregation of human lysozyme variants underlying amyloid fibrillogenesis. *Nature* **385,** 787–793 (1997).
5. Fowler, D. M., Koulov, A. V., Balch, W. E. & Kelly, J. W. Functional amyloid — from bacteria to humans. *Trends Biochem. Sci.* **32,** 217–224 (2007).
6. Hardy, J. & Selkoe, D. J. The amyloid hypothesis of Alzheimer's disease: progress and problems on the road to therapeutics. *Science* **297,** 353–356 (2002).
7. Chiti, F. & Dobson, C. M. Protein misfolding, functional amyloid, and human disease. *Annu. Rev. Biochem.* **75,** 333–366 (2006).
8. Knowles, T. P. J., Vendruscolo, M. & Dobson, C. M. The amyloid state and its association with protein misfolding diseases. *Nature Rev. Mol. Cell Biol.* **15,** 384–396 (2014).
9. Greenwald, J. & Riek, R. Biology of amyloid: structure, function, and regulation. *Structure* **18,** 1244–1260 (2010).
10. Eisenberg, D. & Jucker, M. The amyloid state of proteins in human diseases. *Cell* **148,** 1188–1203 (2012).
11. Eisele, Y. S. *et al.* Targeting protein aggregation for the treatment of degenerative diseases. *Nature Rev. Drug Discov.* **14,** 759–780 (2015).
12. Maury, C. P. J. The emerging concept of functional amyloid. *J. Intern. Med.* **265,** 329–334 (2009).
13. Maji, S. K. *et al*. Functional amyloids as natural storage of peptide hormones in pituitary secretory granules. *Science* **325,** 328–332 (2009).
14. Sunde, M. *et al.* Common core structure of amyloid fibrils by synchrotron X-ray diffraction. *J. Mol. Biol.* 273, 729–739 (1997).
Evidence that amyloid fibrils, in general, are composed of the cross-β-sheet structure.
15. Jiménez, J. L. *et al.* The protofilament structure of insulin amyloid fibrils. *Proc. Natl Acad. Sci. USA* **99,** 9196–9201 (2002).
The first atomic-resolution structures of amyloid-like crystals, which revealed the steric-zipper side-chain motif, including the Asn and Gln hydrogen-bond ladders.
16. Nelson, R. *et al.* Structure of the cross-β spine of amyloid-like fibrils. *Nature* **435,** 773–778 (2005).
17. Sawaya, M. R. *et al.* Atomic structures of amyloid cross-β spines reveal varied steric zippers. *Nature* **447,** 453–457 (2007).
The various classes of cross-β-sheet structures are revealed at atomic resolution.
18. Ivanova, M. I., Sievers, S. A., Sawaya, M. R., Wall, J. S. & Eisenberg, D. Molecular basis for insulin fibril assembly. *Proc. Natl Acad. Sci. USA* **106,** 18990–18995 (2009).
19. Wiltzius, J. J. W., Sievers, S. A., Sawaya, M. R. & Eisenberg, D. Atomic structures of IAPP (amylin) fusions suggest a mechanism for fibrillation and the role of insulin in the process. *Protein Sci.* **18,** 1521–1530 (2009).
20. Wiltzius, J. J. W. *et al.* Molecular mechanisms for protein-encoded inheritance. *Nature Struct. Mol. Biol.* **16,** 973–978 (2009).
21. Colletier, J.-P. *et al.* Molecular basis for amyloid-β polymorphism. *Proc. Natl Acad. Sci. USA* **108,** 16938–16943 (2011).
22. Apostol, M. I., Sawaya, M. R., Cascio, D. & Eisenberg, D. Crystallographic studies of prion protein (PrP) segments suggest how structural changes encoded by polymorphism at residue 129 modulate susceptibility to human prion disease. *J. Biol. Chem.* **285,** 29671–29675 (2010).
23. Apostol, M. I., Wiltzius, J. J. W., Sawaya, M. R., Cascio, D. & Eisenberg, D. Atomic structures suggest determinants of transmission barriers in mammalian prion disease. *Biochemistry* **50,** 2456–2463 (2011).
24. Soriaga, A. B., Sangwan, S., Macdonald, R., Sawaya, M. R. & Eisenberg, D. Crystal structures of IAPP amyloidogenic segments reveal a novel packing motif of out-of-register beta sheets. *J. Phys. Chem. B* **120,** 5810–5816 (2016).
25. Saelices, L. *et al.* Uncovering the mechanism of aggregation of human transthyretin. *J. Biol. Chem.* **290,** 28932–28943 (2015).
26. Rodriguez, J. A. *et al.* Structure of the toxic core of α-synuclein from invisible crystals. *Nature* **525,** 486–490 (2015).
27. Balbirnie, M., Grothe, R. & Eisenberg, D. S. An amyloid-forming peptide from the yeast prion Sup35 reveals a dehydrated β-sheet structure for amyloid. *Proc. Natl Acad. Sci. USA* **98,** 2375–2380 (2001).
28. Tsemekhman, K., Goldschmidt, L., Eisenberg, D. & Baker, D. Cooperative hydrogen bonding in amyloid formation. *Protein Sci.* **16,** 761–764 (2007).
29. Landreh, M. *et al.* The formation, function and regulation of amyloids: insights from structural biology. *J. Intern. Med.* **280,** 164–176 (2016).
30. Liu, C. *et al.* Out-of-register β-sheets suggest a pathway to toxic amyloid aggregates. *Proc. Natl Acad. Sci. USA* **109,** 20913–20918 (2012).
31. van der Wel, P. C. A., Lewandowski, J. R. & Griffin, R. G. Solid-state NMR study of amyloid nanocrystals and fibrils formed by the peptide GNNQQNY from yeast prion protein Sup35p. *J. Am. Chem. Soc.* **129,** 5117–5130 (2007).
32. Schmidt, M. *et al.* Peptide dimer structure in an Aβ(1–42) fibril visualized with cryo-EM. *Proc. Natl Acad. Sci. USA* **112,** 11858–11863 (2015).
The cryo-EM reconstruction of an amyloid-β(1–42) fibril reveals an intermolecular steric-zipper motif.
33. Colvin, M. T. *et al.* Atomic resolution structure of monomorphic Aβ42 amyloid fibrils. *J. Am. Chem. Soc.* **138,** 9663–9674 (2016).
Refs 33 and 34 present the atomic-resolution solid-state NMR structure of an amyloid-β(1–42) fibril associated with AD, revealing hydrophobic interactions in concert with the cross-β-sheet motif as important contributors to the amyloid structure.
34. Wälti, M. A. *et al.* Atomic-resolution structure of a disease-relevant Aβ(1–42) amyloid fibril. *Proc. Natl Acad. Sci. USA* **113,** E4976–E4984 (2016).
35. Xiao, Y. *et al.* Aβ(1–42) fibril structure illuminates self-recognition and replication of amyloid in Alzheimer's disease. *Nature Struct. Mol. Biol.* **22,** 499–505 (2015).
36. Tuttle, M. D. *et al.* Solid-state NMR structure of a pathogenic fibril of full-length human α-synuclein. *Nature Struct. Mol. Biol.* **23,** 409–415 (2016).
A solid-state NMR structure of cell-infectious amyloid fibrils of α-synuclein associated with PD.
37. Terry, C. *et al. Ex vivo* mammalian prions are formed of paired double helical prion protein fibrils. *Open Biol.* **6,** 160035 (2016).
38. Vázquez-Fernández, E. *et al.* The structural architecture of an infectious mammalian prion using electron cryomicroscopy. *PLoS Pathog.* **12,** e1005835 (2016).
39. Groveman, B. R. *et al.* Parallel in-register intermolecular β-sheet architectures for prion-seeded prion protein (PrP) amyloids. *J. Biol. Chem.* **289,** 24129–24142 (2014).
40. Helmus, J. J., Surewicz, K., Nadaud, P. S., Surewicz, W. K. & Jaroniec, C. P. Molecular conformation and dynamics of the Y145Stop variant of human prion protein in amyloid fibrils. *Proc. Natl Acad. Sci. USA* **105,** 6284–6289 (2008).
41. Müller, H. *et al.* Progress towards structural understanding of infectious sheep PrP-amyloid. *Prion* **8,** 344–358 (2014).
42. Jones, E. M. *et al.* Structural polymorphism in amyloids: new insights from studies with Y145Stop prion protein fibrils. *J. Biol. Chem.* **286,** 42777–42784 (2011).

© 2016 Macmillan Publishers Limited, part of Springer Nature. All rights reserved.

43. Coustou, V., Deleu, C., Saupe, S. & Begueret, J. The protein product of the het-s heterokaryon incompatibility gene of the fungus *Podospora anserina* behaves as a prion analog. *Proc. Natl Acad. Sci. USA* **94,** 9773–9778 (1997).
44. Wasmer, C. *et al.* Amyloid fibrils of the HET-s(218–289) prion form a β solenoid with a triangular hydrophobic core. *Science* **319,** 1523–1526 (2008).
The 3D structure of a biological-relevant functional amyloid reveals a β-solenoid helix with two windings per molecules, indicating an evolutionarily-evolved prion.
45. Klabunde, T. *et al.* Rational design of potent human transthyretin amyloid disease inhibitors. *Nature Struct. Biol.* **7,** 312–321 (2000).
46. Vilar, M. *et al.* The fold of α-synuclein fibrils. *Proc. Natl Acad. Sci. USA* **105,** 8637–8642 (2008).
47. Bousset, L. *et al.* Structural and functional characterization of two alpha-synuclein strains. *Nature Commun.* **4,** 2575 (2013).
Two α-synuclein polymorphs with distinct structures at both the atomic and the mesoscopic levels show distinct toxicities.
48. Meinhardt, J., Sachse, C., Hortschansky, P., Grigorieff, N. & Fändrich, M. Aβ(1–40) fibril polymorphism implies diverse interaction patterns in amyloid fibrils. *J. Mol. Biol.* **386,** 869–877 (2009).
49. Ravotti, F. *et al.* Solid-state NMR sequential assignment of an amyloid-β(1–42) fibril polymorph. Biomol. *NMR Assign.* **10,** 269–276 (2016).
50. Tycko, R. Physical and structural basis for polymorphism in amyloid fibrils. *Protein Sci.* **23,** 1528–1539 (2014).
51. Paravastu, A. K., Leapman, R. D., Yau, W.-M. & Tycko, R. Molecular structural basis for polymorphism in Alzheimer's β-amyloid fibrils. *Proc. Natl Acad. Sci. USA* **105,** 18349–18354 (2008).
52. Petkova, A. T. *et al.* Self-propagating, molecular-level polymorphism in Alzheimer's β-amyloid fibrils. *Science* **307,** 262–265 (2005).
The presence of self-propagating polymorphs is revealed at the atomic level using solid-state NMR.
53. Anfinsen, C. B. Principles that govern the folding of protein chains. *Science* **181,** 223–230 (1973).
54. Daskalov, A. *et al.* Contribution of specific residues of the β-solenoid fold to HET-s prion function, amyloid structure and stability. *PLoS Pathog.* **10,** e1004158 (2014).
55. Wang, L., Schubert, D., Sawaya, M. R., Eisenberg, D. & Riek, R. Multidimensional structure-activity relationship of a protein in its aggregated states. *Angew. Chem. Int. Edn Engl.* **49,** 3904–3908 (2010).
56. Silva, J. L., De Moura Gallo, C. V., Costa, D. C. F. & Rangel, L. P. Prion-like aggregation of mutant p53 in cancer. *Trends Biochem. Sci.* **39,** 260–267 (2014).
57. Ano Bom, A. P. D. *et al.* Mutant p53 aggregates into prion-like amyloid oligomers and fibrils: implications for cancer. *J. Biol. Chem.* **287,** 28152–28162 (2012).
58. Soragni, A. *et al.* A designed inhibitor of p53 aggregation rescues p53 tumor suppression in ovarian carcinomas. *Cancer Cell* **29,** 90–103 (2016).
59. Xu, J. *et al.* Gain of function of mutant p53 by coaggregation with multiple tumor suppressors. *Nature Chem. Biol.* **7,** 285–295 (2011).
60. Riek, R. & Saupe, S. J. The HET-S/s prion motif in the control of programmed cell death. *Cold Spring Harb. Perspect. Biol.* **8,** a023515 (2016).
61. Seuring, C. *et al.* The mechanism of toxicity in HET-S/HET-s prion incompatibility. *PLoS Biol.* **10,** e1001451 (2012).
62. Caudron, F. & Barral, Y. A super-assembly of Whi3 encodes memory of deceptive encounters by single cells during yeast courtship. *Cell* **155,** 1244–1257 (2013).
63. Si, K., Choi, Y.-B., White-Grindley, E., Majumdar, A. & Kandel, E. R. Aplysia CPEB can form prion-like multimers in sensory neurons that contribute to long-term facilitation. *Cell* **140,** 421–435 (2010).
64. Si, K., Lindquist, S. & Kandel, E. R. A neuronal isoform of the aplysia CPEB has prion-like properties. *Cell* **115,** 879–891 (2003).
65. Geoghegan, J. C. *et al.* Selective incorporation of polyanionic molecules into hamster prions. *J. Biol. Chem.* **282,** 36341–36353 (2007).
66. Supattapone, S. Elucidating the role of cofactors in mammalian prion propagation. *Prion* **8,** 100–105 (2014).
67. Prusiner, S. B. Prions. *Proc. Natl Acad. Sci. USA* **95,** 13363–13383 (1998).
68. Tanaka, M., Chien, P., Naber, N., Cooke, R. & Weissman, J. S. Conformational variations in an infectious protein determine prion strain differences. *Nature* **428,** 323–328 (2004).
69. Cohen, S. I. A. *et al.* Proliferation of amyloid-β42 aggregates occurs through a secondary nucleation mechanism. *Proc. Natl Acad. Sci. USA* **110,** 9758–9763 (2013).
70. Arosio, P., Knowles, T. P. J. & Linse, S. On the lag phase in amyloid fibril formation. *Phys. Chem. Chem. Phys.* **17,** 7606–7618 (2015).
71. Riek, R. Cell biology: infectious Alzheimer's disease? *Nature* **444,** 429–431 (2006).
72. Meyer-Luehmann, M. *et al.* Exogenous induction of cerebral β-amyloidogenesis is governed by agent and host. *Science* **313,** 1781–1784 (2006).
Demonstrates that aggregates of amyloid-β(1–42) are transmissible in a mouse model of AD.
73. Chernoff, Y. O., Lindquist, S. L., Ono, B., Inge-Vechtomov, S. G. & Liebman, S. W. Role of the chaperone protein Hsp104 in propagation of the yeast prion-like factor [*psi*+]. *Science* **268,** 880–884 (1995).
74. Alper, T., Cramp, W. A., Haig, D. A. & Clarke, M. C. Does the agent of scrapie replicate without nucleic acid? *Nature* **214,** 764–766 (1967).
75. Griffith, J. S. Self-replication and scrapie. *Nature* **215,** 1043–1044 (1967).
76. Prusiner, S. B. Novel proteinaceous infectious particles cause scrapie. *Science* **216,** 136–144 (1982).
77. Serio, T. R. & Lindquist, S. L. [PSI+], SUP35, and chaperones. *Adv. Protein Chem.* **57,** 335–366 (2001).
78. Wickner, R. B. *et al.* Yeast prions act as genes composed of self-propagating protein amyloids. *Adv. Protein Chem.* **57,** 313–334 (2001).
79. Edskes, H. K., Gray, V. T. & Wickner, R. B. The [URE3] prion is an aggregated form of Ure2p that can be cured by overexpression of Ure2p fragments. *Proc. Natl Acad. Sci. USA* **96,** 1498–1503 (1999).
80. Patino, M. M., Liu, J. J., Glover, J. R. & Lindquist, S. Support for the prion hypothesis for inheritance of a phenotypic trait in yeast. *Science* **273,** 622–626 (1996).
81. Castilla, J., Saá, P., Hetz, C. & Soto, C. *In vitro* generation of infectious scrapie prions. *Cell* **121,** 195–206 (2005).
82. Wang, F., Wang, X., Yuan, C.-G. & Ma, J. Generating a prion with bacterially expressed recombinant prion protein. *Science* **327,** 1132–1135 (2010).
83. Ritter, C. *et al.* Correlation of structural elements and infectivity of the HET-s prion. *Nature* **435,** 844–848 (2005).
84. Jucker, M. & Walker, L. C. Pathogenic protein seeding in Alzheimer disease and other neurodegenerative disorders. *Ann. Neurol.* **70,** 532–540 (2011).
85. Walsh, D. M. & Selkoe, D. J. A critical appraisal of the pathogenic protein spread hypothesis of neurodegeneration. *Nature Rev. Neurosci.* **17,** 251–260 (2016).
86. Morales, R., Bravo-Alegria, J., Duran-Aniotz, C. & Soto, C. Titration of biologically active amyloid-β seeds in a transgenic mouse model of Alzheimer's disease. *Sci. Rep.* **5,** 9349 (2015).
87. Wu, J. W. *et al.* Neuronal activity enhances tau propagation and tau pathology *in vivo*. *Nature Neurosci.* **19,** 1085–1092 (2016).
88. Luk, K. C. *et al.* Pathological α-synuclein transmission initiates Parkinson-like neurodegeneration in nontransgenic mice. *Science* **338,** 949–953 (2012).
89. Lundmark, K. *et al.* Transmissibility of systemic amyloidosis by a prion-like mechanism. *Proc. Natl Acad. Sci. USA* **99,** 6979–6984 (2002).
90. Jaunmuktane, Z. *et al.* Evidence for human transmission of amyloid-β pathology and cerebral amyloid angiopathy. *Nature* **525,** 247–250 (2015).
Demonstrates that amyloid-β(1–42) pathology is transmissible in humans.
91. Ridley, R. M., Baker, H. F., Windle, C. P. & Cummings, R. M. Very long term studies of the seeding of β-amyloidosis in primates. *J. Neural Transm.* **113,** 1243–1251 (2006).
92. Lu, J.-X. *et al.* Molecular structure of β-amyloid fibrils in Alzheimer's disease brain tissue. *Cell* **154,** 1257–1268 (2013).
93. Aguzzi, A. & Lakkaraju, A. K. K. Cell biology of prions and prionoids: a status report. *Trends Cell Biol.* **26,** 40–51 (2016).
94. Aguzzi, A. & Rajendran, L. The transcellular spread of cytosolic amyloids, prions, and prionoids. *Neuron* **64,** 783–790 (2009).
95. Weissmann, C. Birth of a prion: spontaneous generation revisited. *Cell* **122,** 165–168 (2005).
96. Asante, E. A. *et al.* BSE prions propagate as either variant CJD-like or sporadic CJD-like prion strains in transgenic mice expressing human prion protein. *EMBO J.* **21,** 6358–6366 (2002).
97. Cali, I. *et al*. Co-existence of scrapie prion protein types 1 and 2 in sporadic Creutzfeldt-Jakob disease: its effect on the phenotype and prion-type characteristics. *Brain* **132,** 2643–2658 (2009).
98. Sigurdson, C. J. *et al.* Prion strain discrimination using luminescent conjugated polymers. *Nature Methods* **4,** 1023–1030 (2007).
99. Cali, I. *et al.* Classification of sporadic Creutzfeldt-Jakob disease revisited. *Brain* **129,** 2266–2277 (2006).
100. King, C.-Y. & Diaz-Avalos, R. Protein-only transmission of three yeast prion strains. *Nature* **428,** 319–323 (2004).
101. Toyama, B. H., Kelly, M. J. S., Gross, J. D. & Weissman, J. S. The structural basis of yeast prion strain variants. *Nature* **449,** 233–237 (2007).
102. Li, J., Browning, S., Mahal, S. P., Oelschlegel, A. M. & Weissmann, C. Darwinian evolution of prions in cell culture. *Science* **327,** 869–872 (2010).
Evidence for the adaptation of prions.
103. Weissmann, C., Li, J., Mahal, S. P. & Browning, S. Prions on the move. *EMBO Rep.* **12,** 1109–1117 (2011).
104. Oelschlegel, A. M. & Weissmann, C. Acquisition of drug resistance and dependence by prions. *PLoS Pathog.* **9,** e1003158 (2013).
105. Collinge, J. & Clarke, A. R. A general model of prion strains and their pathogenicity. *Science* **318,** 930–936 (2007).
106. Eigen, M. Selforganization of matter and the evolution of biological macromolecules. *Naturwissenschaften* **58,** 465–523 (1971).
107. Spillantini, M. G. *et al.* α-Synuclein in Lewy bodies. *Nature* **388,** 839–840 (1997).
108. Goldgaber, D., Lerman, M. I., McBride, O. W., Saffiotti, U. & Gajdusek, D. C. Characterization and chromosomal localization of a cDNA encoding brain amyloid of Alzheimer's disease. *Science* **235,** 877–880 (1987).
109. Tanzi, R. E. *et al.* Amyloid beta protein gene: cDNA, mRNA distribution, and genetic linkage near the Alzheimer locus. *Science* **235,** 880–884 (1987).
110. Suzuki, N. *et al.* An increased percentage of long amyloid beta protein secreted by familial amyloid beta protein precursor (beta APP717) mutants. *Science* **264,** 1336–1340 (1994).
111. Birk, J., Friberg, M. A., Prescianotto-Baschong, C., Spiess, M. & Rutishauser, J. Dominant pro-vasopressin mutants that cause diabetes insipidus form disulfide-linked fibrillar aggregates in the endoplasmic reticulum. *J. Cell Sci.* **122,** 3994–4002 (2009).
112. Chesebro, B. *et al.* Anchorless prion protein results in infectious amyloid disease without clinical scrapie. *Science* **308,** 1435–1439 (2005).
113. Sandberg, M. K., Al-Doujaily, H., Sharps, B., Clarke, A. R. & Collinge, J. Prion propagation and toxicity *in vivo* occur in two distinct mechanistic phases. *Nature* **470,** 540–542 (2011).

© 2016 Macmillan Publishers Limited, part of Springer Nature. All rights reserved.

114. Walsh, D. M. & Selkoe, D. J. Aβ oligomers — a decade of discovery. *J. Neurochem.* **101,** 1172–1184 (2007).
115. Hardy, J. A. & Higgins, G. A. Alzheimer's disease: the amyloid cascade hypothesis. *Science* **256,** 184–185 (1992).
116. Silveira, J. R. *et al.* The most infectious prion protein particles. *Nature* **437,** 257–261 (2005).
117. Pieri, L., Madiona, K., Bousset, L. & Melki, R. Fibrillar α-synuclein and huntingtin exon 1 assemblies are toxic to the cells. *Biophys. J.* **102,** 2894–2905 (2012).
118. Jarrett, J. T. & Lansbury, P. T. Seeding 'one-dimensional crystallization' of amyloid: a pathogenic mechanism in Alzheimer's disease and scrapie? *Cell* **73,** 1055–1058 (1993).
119. Lashuel, H. A., Hartley, D., Petre, B. M., Walz, T. & Lansbury, P. T. Neurodegenerative disease: amyloid pores from pathogenic mutations. *Nature* **418,** 291 (2002).
120. Abedini, A. *et al.* Time-resolved studies define the nature of toxic IAPP intermediates, providing insight for anti-amyloidosis therapeutics. *eLife* **5,** e12977 (2016).
121. Cohen, S. I. A. *et al.* A molecular chaperone breaks the catalytic cycle that generates toxic Aβ oligomers. *Nature Struct. Mol. Biol.* **22,** 207–213 (2015).
122. Laganowsky, A. *et al.* Atomic view of a toxic amyloid small oligomer. *Science* **335,** 1228–1231 (2012).
123. Jan, A. *et al.* Aβ42 neurotoxicity is mediated by ongoing nucleated polymerization process rather than by discrete Aβ42 species. *J. Biol. Chem.* **286,** 8585–8596 (2011).
124. Reynolds, N. P. *et al.* Mechanism of membrane interaction and disruption by α-synuclein. *J. Am. Chem. Soc.* **133,** 19366–19375 (2011).
125. Ankarcrona, M. *et al.* Current and future treatment of amyloid diseases. *J. Intern. Med.* **280,** 177–202 (2016).
126. Knight, S. D., Presto, J., Linse, S. & Johansson, J. The BRICHOS domain, amyloid fibril formation, and their relationship. *Biochemistry* **52,** 7523–7531 (2013).
127. Johnson, S. M., Connelly, S., Fearns, C., Powers, E. T. & Kelly, J. W. The transthyretin amyloidoses: from delineating the molecular mechanism of aggregation linked to pathology to a regulatory-agency-approved drug. *J. Mol. Biol.* **421,** 185–203 (2012).
A review on the successful development of a drug through stabilizing the native form of the amyloid protein.
128. Eisenberg, D. S. & Sawaya, M. R. Implications for Alzheimer's disease of an atomic resolution structure of amyloid-β(1–42) fibrils. *Proc. Natl Acad. Sci. USA* **113,** 9398–9400 (2016).
129. Sunde, M. & Blake, C. The structure of amyloid fibrils by electron microscopy and X-ray diffraction. *Adv. Protein Chem.* **50,** 123–159 (1997).
130. Astbury, W. T., Dickinson, S. & Bailey, K. The X-ray interpretation of denaturation and the structure of the seed globulins. *Biochem. J.* **29,** 2351–2360 (1935).
The cross-β-sheet structure is introduced on the basis of X-ray fibre diffraction studies of protein aggregates induced by heat denaturation.
131. Asakura, S. Polymerization of flagellin and polymorphism of flagella. *Adv. Biophys.* **1,** 99–155 (1970).
132. Oosawa, F. & Asakura, S. *Thermodynamics of the Polymerization of Protein* (Academic, 1975).
133. Bishop, M. F. & Ferrone, F. A. Kinetics of nucleation-controlled polymerization. A perturbation treatment for use with a secondary pathway. *Biophys. J.* **46,** 631–644 (1984).
134. Pronchik, J., He, X., Giurleo, J. T. & Talaga, D. S. *In vitro* formation of amyloid from α-synuclein is dominated by reactions at hydrophobic interfaces. *J. Am. Chem. Soc.* **132,** 9797–9803 (2010).
135. Campioni, S. *et al.* The presence of an air-water interface affects formation and elongation of α-synuclein fibrils. *J. Am. Chem. Soc.* **136,** 2866–2875 (2014).
136. Knowles, T. P. J. *et al.* An analytical solution to the kinetics of breakable filament assembly. *Science* **326,** 1533–1537 (2009).
137. Hurshman, A. R., White, J. T., Powers, E. T. & Kelly, J. W. Transthyretin aggregation under partially denaturing conditions is a downhill polymerization. *Biochemistry* **43,** 7365–7381 (2004).

Acknowledgements We thank K. Comiotto and M. Sawaya for making figures and the Swiss National Science Foundation (SNSF), the US National Institutes of Health and the Howard Hughes Medical Institute for continuing support of our research, including an SNSF Sinergia grant to R.R.

Author Information Reprints and permissions information is available at www.nature.com/reprints. The authors declare no competing financial interests. Readers are welcome to comment on the online version of this paper at go.nature.com/2f8daq7. Correspondence should be addressed to R.R. (roland.riek@phys.chem.ethz.ch) and D.S.E. (david@mbi.ucla.edu).

Reviewer Information *Nature* thanks G. Pielak and the other anonymous reviewer(s) for their contribution to the peer review of this work.

© 2016 Macmillan Publishers Limited, part of Springer Nature. All rights reserved.